

PAPER • OPEN ACCESS

Atelocollagen-based hydrogel loaded with *Cotinus coggygria* extract for treatment of type 2 diabetic wounds

To cite this article: Candan Yilmaz Ozdogan *et al* 2025 *Biomed. Mater.* **20** 025009

View the [article online](#) for updates and enhancements.

You may also like

- [Development of a 3D cell printed construct considering angiogenesis for liver tissue engineering](#)
Jin Woo Lee, Yeong-Jin Choi, Woon-Jae Yong *et al.*
- [Biomimetic human skin model patterned with rete ridges](#)
Maxwell B Nagarajan, Alexander J Ainscough, Daniel S Reynolds *et al.*
- [Local extensional flows promote long-range fiber alignment in 3D collagen hydrogels](#)
Adeel Ahmed, Mehran Mansouri, Indranil M Joshi *et al.*



GCAS

BreathSpec®

The combination of GC and IMS enables a physical separation to detect volatiles without pre-concentration directly sampled from human breath.

Our GC-IMS based analyzer allows instant breath sampling and analysis of volatiles in minutes.

The transportable GC-IMS facilitates versatile sampling incl. direct exhalation, syringe based and also gas bags for sampling of breath and static body headspace (oral/nasal/skin).

▶▶▶ [click for more details](#)

Biomedical Materials



PAPER

Atelocollagen-based hydrogel loaded with *Cotinus coggygria* extract for treatment of type 2 diabetic wounds

OPEN ACCESS

RECEIVED

13 June 2024

REVISED

21 December 2024

ACCEPTED FOR PUBLICATION

8 January 2025

PUBLISHED

24 January 2025

Original content from this work may be used under the terms of the [Creative Commons Attribution 4.0 licence](https://creativecommons.org/licenses/by/4.0/).

Any further distribution of this work must maintain attribution to the author(s) and the title of the work, journal citation and DOI.



Candan Yilmaz Ozdogan^{1,2,*} , Halime Kenar^{3,4} , Huseyin Uzuner^{2,5} and Aynur Karadenizli²

¹ Department of Medical Biology, Diabetes and Obesity Research Laboratory, Faculty of Medicine, Kocaeli University, Kocaeli, Turkey

² Department of Medical Microbiology, Molecular Research and Antibody Laboratory, Faculty of Medicine, Kocaeli University, Kocaeli, Turkey

³ Department of Biomedical Engineering, Faculty of Engineering and Natural Sciences, Acibadem Mehmet Ali Aydinlar University, Istanbul, Turkey

⁴ ACU Biomaterials A & R Center, Acibadem Mehmet Ali Aydinlar University (ACU), Istanbul, 34752, Turkey

⁵ Department of Medical Services and Techniques, Kocaeli Vocational School of Health Services, Kocaeli University, Kocaeli, Turkey

* Author to whom any correspondence should be addressed.

E-mail: candan.ozdogan@kocaeli.edu.tr

Keywords: atelocollagen, *Cotinus coggygria*, dermal fibroblasts, diabetic wound healing, wound dressing

Abstract

Diabetes, a chronic metabolic disease, causes complications such as chronic wounds, which are difficult to cure. New treatments have been investigated to accelerate wound healing. In this study, a novel wound dressing from fibroblast-laden atelocollagen-based hydrogel with *Cotinus coggygria* extract was developed for diabetic wound healing. The antimicrobial activity of *C. coggygria* hexane (H), dichloromethane (DCM), dichloromethane:methanol (DCM-M), methanol (M), distilled water (DW) and traditional (T) extracts against *Staphylococcus aureus*, *Escherichia coli*, *Pseudomonas aeruginosa*, *Enterococcus faecalis* and *Candida albicans*, as well as their cytotoxic effects on fibroblasts were determined. While fibroblast growth was significantly ($p < 0.05$) promoted with DCM ($121.41 \pm 1.04\%$), M ($109.40 \pm 5.89\%$) and DW ($121.83 \pm 6.37\%$) extracts at their lowest concentrations, $2000 \mu\text{g ml}^{-1}$ DCM and $7.8 \mu\text{g ml}^{-1}$ T extracts had both non-cytotoxic and antifungal effects. An atelocollagen-based hydrogel was produced by thermal crosslinking, and its pore size ($38.75 \pm 7.67 \mu\text{m}$), water content ($96.63 \pm 0.24\%$) and swelling ratio ($27.21 \pm 4.08\%$) were found to be suitable for wound dressings. A significant increase in the deoxyribonucleic acid amount ($28.27 \pm 1.41\%$) was observed in the plain hydrogel loaded with fibroblasts after 9 d of incubation, and the hydrogel had an extensively interconnected cellular network. The hydrogels containing DW and T extracts were applied to wounds generated in an *in vitro* 3D type-2-diabetic human skin model. Although the incubation period was not sufficient for closure of the wounds in either of the treatments, the hydrogel with T extract stimulated more fibroblast migration. In the fibroblast-laden version of the hydrogel with T extract, no wound closure was observed but more keratinocytes migrated to the wound region. These positive outcomes underline the potential of the developed wound dressing as a powerful alternative to improve diabetic wound healing in clinical practice.

1. Introduction

Diabetes is a chronic metabolic disease characterized by a high glucose concentration in the blood, which may affect more than 783 million adults globally by 2045 [1–3]. There are two major classes of diabetes: type 1 and type 2. While type 1 diabetes encompasses defects or a complete absence of insulin secretion,

cells do not respond to insulin correctly in type 2 diabetes. Studies have shown that type 2 diabetes is more prevalent than type 1 diabetes [4]. Diabetic foot ulcers, the most devastating complication of diabetes, remain a great challenge for clinicians due to the long treatment duration, as well as the overwhelming economic burden for society [3, 5]. Diabetic chronic wounds affect 25% of diabetic patients, nearly 30% of

whom require amputation as treatment. This means that every 20 s, a diabetic patient suffers a lower limb amputation [4, 5].

Wound healing is a complex process with four overlapping phases: hemostasis, inflammation, proliferation and remodeling. It requires the activation, recruitment or activity of inflammatory cells, fibroblasts, keratinocytes and endothelial cells, as well as related growth factors and enzymes [6]. However, diabetic wounds do not proceed through these four stages of normal wound healing [2]. Wound healing in diabetes has been characterized by impaired healing, bacterial infection, oxidative stress, prolonged inflammation and reduced epithelialization kinetics [7, 8]. Currently, the treatments for diabetic wounds include systemic strategies [5], hyperbaric oxygen therapy [9], electrical stimulation, application of various topical wound dressings and cell-based therapies, and the use of dermal and epidermal skin substitutes [8]. In addition, scientists have had a continued interest in traditional folk medicines for many years, as plants, a source of many bioactive compounds, have less deleterious side effects than synthetic drugs [10, 11]. Secondary metabolites, such as tannins, terpenoids, alkaloids and flavonoids produced by higher plants are an abundant source of biologically active compounds that could be a basis for the development of new chemicals for pharmaceuticals [10]. The plant *Cotinus coggygria*, from the family of Anacardiaceae, is one of these medicinal plants. It is a large shrub or small tree that is found from Southern Europe, the Mediterranean, Moldova and the Caucasus to central China to the Himalayas [10, 12]. It has been reported to possess potential antioxidant, anti-inflammatory, anti-hemorrhagic, hepatoprotective, anti-ulcerogenic, wound healing and immunostimulant effects as well as antimicrobial activity [12, 13]. Phytochemical investigation of the plant's different parts has resulted in the isolation of flavonoids (fisetin, fustin, quercetin, apigenin, myricetin, taxifolin), aurones (sulfuretin, disulfuretin, sulfurein), chalcones (butein, isoliquiritigenin), anthocyanins (delphinidin-3-galactoside, cyanidin-3-galactoside, petunidin-3-glucoside), catechins and other phenolics, e.g. gallic acid and methyl gallate [14].

Selecting an appropriate wound healing strategy by considering the condition of the wound is critical for successful healing, since this can enhance the speed of wound healing by minimizing the risk of complications and scar formation. Cell therapy, a simple, less time consuming and less invasive therapeutic approach, is effective in improving wound healing without the need for major surgical procedures or donor-site morbidity. This technique can be applied to both acute and chronic wounds and provide tissue that is similar to the surrounding skin,

causing minimal scars and color mismatch. In clinical medicine, a variety of cell types such as fibroblasts, keratinocytes and adipose-derived stromal vascular fraction are used actively. Among them, fibroblast therapy has attracted attention in the treatment of chronic wounds as fibroblasts produce three-dimensional extracellular matrix and secrete various cytokines and growth factors that control the cell proliferation, induce angiogenesis, and modify the inflammatory process [15]. Han *et al* [16] applied freshly isolated fibroblasts to patients with diabetic foot ulcers, and after eight weeks complete wound closure was achieved in 83% of the patients. In a clinical trial, it was proven that the autologous fibroblast-hyaluronic acid complex healed 84% of diabetic foot ulcers without any adverse effects [17]. In another study, patients with ulcers of longer than six weeks duration showed a significant higher percentage of wound closure by week 12 after the application of a human fibroblast-derived dermis (Dermagraft) [18].

Numerous wound dressings involving electrospun membranes, porous foams and functional hydrogels have been developed to act as a physical barrier against mechanical trauma, to protect the injury from infection and to promote the healing process [5, 7, 19]. Because of the high porosity, biocompatibility and functionality and their similarity to biological soft tissues, hydrogels are among the most remarkable dressings for wound healing and skin regeneration [5, 7]. Hydrogels have been dominant alternatives to traditional wound dressings, overcoming their disadvantages such as low flexibility and high adherence to the wound surface, frequently associated with painful removal. The swelling property of hydrogels provides a favorable moist environment for wound healing and a porous structure that allows wound exudate absorption and oxygen permeation, thus promoting keratinocyte migration and fibroblast proliferation. Furthermore, the hydrogels efficiently support hemostasis and provide long-term protection for the wounds [2, 5, 19]. Single-function hydrogels usually fail to support complete healing because of the multifactor nature of diabetic wounds. It is possible to develop hydrogels as multifunctional dressings that are loaded with active compounds such as growth factors for the stimulation of cell proliferation and tissue repair, and antimicrobials for the inhibition of bacterial growth and prevention of microbial infection [6, 19]. Collagen, the most abundant protein found in the body, has been applied as an adjunct therapy in wound healing. It can support healing by acting as a sink for the ranging matrix metalloproteinases (MMPs) and other enzymes in the wound area, thereby decreasing the intensity of inflammation and restoring progression into the reparative stages. Furthermore, collagen promotes a proangiogenic, anti-inflammatory

environment to aid healing [20]. In tissue engineering, animal-derived collagen is mostly used, and hence may cause immunogenic reactions in humans. Atelocollagen as a low immunogenic derivative of collagen has been developed by the removal of N- and C-terminal telopeptide components in order to prevent these reactions [21]. In regenerative medicine, an attractive approach is the delivery of cells in solubilized collagen through minimally invasive techniques to fill defects. The collagen solution can spontaneously gel through hydrophobic bonding induced by a rise in temperature or pH as the defect is filled [22]. Because these spontaneous gels are mechanically weak and easily deformed, different polymers are added to improve their mechanical properties. Among them, the linear anionic polysaccharide sodium alginate, which exists widely in many species of brown seaweeds, has been studied extensively due to its nontoxicity and compatibility [23]. In the presence of certain divalent cations, such as Ca^{2+} , sodium alginate forms stable gels at room temperature. Calcium crosslinked sodium alginate has been implanted in both animals and humans as a hemostatic wound dressing material [24]. Ascorbic acid is a highly effective antioxidant, acts as an enzyme cofactor for biosynthesis of collagen, has an anti-inflammatory effect, and therefore can cure wounds [25].

In the present study, we aimed to develop a novel wound dressing from atelocollagen-based hydrogel with *C. coggygia* extract, which can be applied together with cellular therapy for diabetic wound healing. The novelty of this work is the determination of the effects of different extracts of *C. coggygia* on the proliferation of fibroblasts obtained from type 2 diabetic patients, their antimicrobial properties against bacteria and fungus commonly encountered in diabetic wounds, and finally the development of a diabetic wound treatment modality from the most potent extract of *C. coggygia*. The antimicrobial activity of different *C. coggygia* extracts against *Staphylococcus aureus*, *Escherichia coli*, *Pseudomonas aeruginosa*, *Enterococcus faecalis* and *Candida albicans*, and their cytotoxic effects on human dermal fibroblasts were determined. Sodium alginate, ascorbic acid and human dermal fibroblasts were blended with atelocollagen derived from bovine tendons. The hydrogels were fabricated by thermal crosslinking, and appropriate cell loading concentrations were determined. An artificial wound was generated at the center of an *in vitro* 3D type 2 diabetic human skin model (DHSM) and treated with atelocollagen-based hydrogel containing *C. coggygia* extracts to evaluate wound healing. After determining which hydrogel type was most effective in the promotion of healing, fibroblasts were also loaded into this hydrogel to evaluate the effect of cell-laden hydrogel therapy on diabetic wound healing.

2. Materials and methods

2.1. Primary cell isolation and culture

All tissue specimens were obtained from donors aged 18–36, who had no genetic diseases. In addition, type 2 diabetic donors were diagnosed with diabetes at least 4 years ago. All protocols involving donors were conducted in adherence to the Declaration of Helsinki.

2.1.1. Isolation and expansion of dermal fibroblasts

Dermal fibroblasts were isolated from skin regarded as medical waste after a second Cesarean delivery according to a previously reported protocol [21]. The skin specimens were obtained from normoglycemic and type 2 diabetic donors. Following skin specimen collection in Hank's Balanced Salt Solution (HBSS, Thermo Scientific) with penicillin/streptomycin (pen/strep), fat and epidermal parts were separated mechanically from the skin. The dermis was cut into small pieces ($3 \times 3 \text{ mm}^2$) by scalpel and cultured on six-well culture plates in Dulbecco's modified Eagle medium: nutrient mixture F-12 (DMEM/F-12) ((1:1 v/v), Thermo Scientific) medium supplemented with 5% human plasma (HP), 2 U ml^{-1} heparin, 1% pen/strep (Lonza) and 1 ng ml^{-1} basic fibroblast growth factor (bFGF, Biologend) as an explant. The cells were grown in medium supplemented with human blood plasma instead of fetal bovine serum to mimic the natural environment of human cells [26]. They were harvested and transferred into a T25 flask after forming a 70% confluency. After the third passage, the cells were characterized by immunostaining for vimentin. The cells that were fixed with 4% formaldehyde were washed with Dulbecco's phosphate-buffered saline (DPBS, Thermo Scientific) and permeabilized with 0.1% triton X-100 (Sigma) for 15 min at room temperature. The cells were then blocked with bovine serum albumin (BSA, Sigma) for 30 min and incubated with anti-vimentin primary antibody (Abcam, 1:100 dilution) overnight at 4°C . After washing with DPBS, the cells were labeled with Alexa fluor 488-conjugated secondary antibody (Thermo Scientific, 1:200 dilution) for 45 min at 37°C . The cells were finally stained with DAPI (Santa Cruz Biotech., 1:1000 dilution) for 10 min at room temperature and were observed under an inverted fluorescence microscope (Olympus IX53 inverted microscope).

2.1.2. Isolation and expansion of keratinocytes

Keratinocytes were isolated from skin pieces of type 2 diabetic donors obtained after reduction mammaplasty surgery according to a previously reported protocol [21]. Skin specimens were taken to the laboratory in HBSS with 2% pen/strep, cleaned with DPBS, and fat portions were removed by scalpel. The skins were cut into 10 mm pieces and were incubated first

overnight at 4 °C in 0.25% trypsin-EDTA (Gibco) and then at 37 °C for 2 h by shaking simultaneously at 135 rpm to separate the epidermal and dermal layers. At the end of incubation, the epidermal and dermal layers were separated mechanically. The epidermal layer was incubated in Cascade medium (Thermo Scientific) for 1 h at 37 °C, filtered by a cell strainer (100 µm), and centrifuged at 1500 rpm. The isolated cells were transferred into T75 flasks coated with an extracellular matrix of human umbilical vein endothelial cells (HUVECs) and cultured in Cascade medium supplemented with 1% keratinocytes growth supplement, 10% HP, 2 U ml⁻¹ heparin and 1% pen/strep in a CO₂ incubator at 37 °C. The characterization of the cells was done by immunostaining for cytokeratin 5. The cells were fixed with 4% formaldehyde, washed with DPBS and permeabilized with 0.1% Triton X-100 for 15 min. After being blocked with BSA, the cells were incubated in 1:500 diluted primary antibody solution (anti-cytokeratin 5 rabbit polyclonal, STJ) overnight at 4 °C, and then were treated with Alexa fluor 568-conjugated secondary antibody (Thermo Scientific, 1:200 dilution) for 1 h at 37 °C. The cell nuclei were counterstained with DAPI and were examined with an inverted fluorescence microscope.

2.1.3. Isolation and expansion of HUVECs

HUVECs were isolated enzymatically as previously reported [21]. Human umbilical cords were collected from type 2 diabetic donors. Briefly, after washing the umbilical cords with DPBS, the umbilical vein was filled with 0.1% collagenase type I (from *Clostridium histolyticum*, Thermo Scientific) prepared in HBSS. The umbilical cord was incubated in a shaking water bath at 37 °C for 25 min, and then the enzyme solution containing the endothelial cells was collected and centrifuged at 1300 rpm for 5 min. The cells were transferred into a gelatin-coated T25 flask and cultured in the 5% CO₂ incubator at 37 °C after being resuspended in endothelial cell growth medium-2 (EGM-2, Lonza) containing 5% HP, 2 U ml⁻¹ heparin and 1% pen/strep. After the second passage, the cells were characterized by immunostaining for CD31. The fixed cells were permeabilized with 0.1% triton X-100 and blocked with BSA for 30 min at room temperature. Then, the cells were incubated with anti-CD31 primary antibody (Dako, 1:50 dilution) overnight at 4 °C, washed with DPBS and labeled with Alexa fluor 488-conjugated secondary antibody (1:200 dilution) for 45 min at 37 °C. After counterstaining with DAPI, the cells were observed under an inverted fluorescence microscope.

2.2. Antimicrobial and cytotoxicity studies of *C. coggygia* extracts

2.2.1. Preparation of plant extracts

The leaves of *C. coggygia* used in the study were collected from Ankara, Turkey, after the tree bloomed.

Plant materials were washed in running tap water and dried at room temperature in the dark. The dried plant leaves were crushed into small pieces and stored at 4 °C in the dark until use. To prepare the hexane (H), dichloromethane (DCM), dichloromethane:methanol (DCM-M), methanol (M) and distilled water (DW) extracts of *C. coggygia*, firstly, the dried and crushed plant leaves (6.67 g l⁻¹) were extracted in hexane (N-hexane for liquid chromatography, Merck), and left at room temperature for 24 h in the dark. Then, the macerated mixture was filtered. The extracts were collected using a rotary evaporator (Buchi rotavapor RII) and lyophilized (hexane extract of *C. coggygia*). After the first filtration, the sediment was treated twice more with the hexane under the same conditions. After the hexane treatment, the leaves of *C. coggygia* were dried completely and the same procedure given above was performed sequentially with dichloromethane (dichloromethane for liquid chromatography, Merck), dichloromethane:methanol (1:1 v/v) (methanol gradient grade for liquid chromatography, Merck), methanol and distilled water. The treatment with each of the solvents was done for 24 h at room temperature in the dark. The traditional extract of *C. coggygia* (T) was prepared by the extraction method used in folk medicine. Briefly, the dried leaves (25 g l⁻¹) were boiled in the distilled water for 20 min and the macerated mixture was filtered, frozen at -20 °C and lyophilized. At the end of the lyophilization, the extracts were stored at -20 °C. Each of the extracts was used within a week.

2.2.2. Antimicrobial properties of *C. coggygia* extracts

The antimicrobial activities of the *C. coggygia* extracts were determined by the broth microdilution method against four strains of bacteria and one strain of yeast that are common micro-organisms seen in diabetic foot ulcers [27, 28]. Standard strains of *S. aureus* (ATCC 29213), *E. coli* (ATCC 25922), *P. aeruginosa* (ATCC 27853), *E. faecalis* (ATCC 29212) and *C. albicans* (ATCC 90028) were used during the experiments. Minimal inhibitory concentrations (MICs) were determined according to the Clinical and Laboratory Standards Institute (CLSI)-M100 for bacteria and CLSI-M27 for yeast. Microdilution tests were performed in Mueller Hinton broth (MHB, Oxoid, UK) for bacterial strains and in RPMI 1640 (Sigma, USA) for yeast. The final concentrations of 1 × 10⁸ CFU ml⁻¹ for bacteria, and 1 × 10⁶ CFU ml⁻¹ for yeast were prepared in the corresponding media. Then, serial dilutions of 1:100 for yeast and 1:10 for bacteria were prepared. Hexane, dichloromethane, dichloromethane:methanol (1:1 v/v), methanol, distilled water and traditional extracts of *C. coggygia* were tested. Two-fold serial dilutions were applied to all extracts at concentrations ranging from 2000 to 7.8 µg ml⁻¹.

MHB and RPMI 1640 were used as diluents in serial dilutions. A total of 100 μl extract was added to each well of a U-bottom 96-well plate. The plates were incubated at 37 °C for 24 h and were examined for the visible growth of bacteria. The lowest concentrations of the extracts without visible growth were defined as the MICs that inhibited microbial growth [29].

2.2.3. Cytotoxic activity of the plant extracts on type 2 diabetic human dermal fibroblasts

The cytotoxic effects of different *C. coggygia* extracts (hexane, dichloromethane, dichloromethane:methanol, methanol, distilled water and traditional extracts) on type 2 diabetic human dermal fibroblasts (T2-HDFs) were evaluated by methylthiazolyldiphenyl-tetrazolium bromide assay (MTT assay, Sigma). Dimethyl sulfoxide (DMSO) was used as the solvent for hexane, dichloromethane:methanol, methanol extracts; DMEM-F12 medium was used for distilled water and traditional extracts, and ethanol (Merck) was used as solvent for the dichloromethane extract. Different concentrations of these plant extracts (2000, 1500, 1000, 500, 250, 150, 100, 50, 25, 12.5 and 7.8 $\mu\text{g ml}^{-1}$) were prepared from their stock solutions in suitable solvents. T2-HDFs were seeded into a 96-well culture plate at a density of 5×10^3 cells/well. Twenty-four hours later, after cell adhesion, the plant extracts were added to the wells and the cells were grown for 4 d. Nutrient medium, DMSO and ethanol in nutrient medium were applied to the wells as control groups. The nutrient medium was DMEM-F12 medium supplemented with 1% L-glutamine, 5% HP, 2 U ml^{-1} heparin, 1 ng ml^{-1} bFGF and 1% pen/strep. At the end of the period, the cells were incubated in DMEM-F12 medium containing 10% MTT reagent for 4 h in a humidified 5% CO_2 incubator at 37 °C. The purple formazan crystals were solubilized by adding DMSO. The plates were analyzed using a microplate reader at a wavelength of 570 nm to measure the optical density (OD) of each well. The percentage of the cell viability (CV) was calculated using the formula given below [30]:

$$\text{CV (\%)} = (\text{Absorbance of sample}/\text{Absorbance of control}) \times 100.$$

The percent cell viability versus plant extract concentration graph was plotted. All experiments were done in triplicate.

According to the results of cytotoxicity and antimicrobial studies, the best *C. coggygia* extract concentration, the one that was noncytotoxic to fibroblasts and showed an antimicrobial effect, was determined.

2.3. Development of the atelocollagen-based hydrogel

2.3.1. Prehydrogel preparation

A solution of bovine Achilles tendon atelocollagen (10 mg ml^{-1}) was prepared in 0.05% acetic acid. A total of 40 mg ml^{-1} of L-ascorbic acid (Sigma) and 10 mg ml^{-1} of sodium alginate (Alginic acid sodium salt from brown algae, Sigma) were prepared in 10XDPBS and in DPBS, respectively. The solution of bovine Achilles tendon collagen, L-ascorbic acid and sodium alginate (4:1:1 v/v/v) was mixed gently from stock solutions (prehydrogel solution) and neutralized by adding NaOH (1 M).

2.3.1.1. Gelation kinetics

The prehydrogel solution was added to a 96-well plate at 150 μl /well and placed into a microplate reader (PerkinElmer, Victor Nivo, USA) prewarmed to 37 °C, and then the absorbance at 405 nm was recorded every 2 min for a total of 60 min. The gelation time of the hydrogels was determined according to the change in turbidity [31].

2.3.1.2. Rheological measurement

Rheological measurements were performed using a KINEXUS Pro Rheometer (Malvern, UK). A thermal crosslinking reaction of the prehydrogel at 37 °C was performed by recording both the elastic modulus (G') and viscous modulus (G''), depending on the time, at 1 Hz with 1% strain [32].

2.3.2. Characterization of the hydrogel

A prehydrogel solution was prepared by following the protocol mentioned in section 2.3.1. The solution was transferred to a 96-well plate (150 μg /well) and incubated for 1 h at 37 °C.

2.3.2.1. Measurement of the swelling ratio

The swelling ratio was determined according to the literature [33]. The hydrogels (W_D) were incubated in DMEM-F12 medium for 24 h at 37 °C to reach the swelling equilibrium (W_W). The swelling ratio of the hydrogels was calculated via the following equation:

$$\text{Swelling ratio (\%)} = ((W_W - W_D)/W_D) \times 100.$$

The swelling ratio was determined from the average values of five measurements.

2.3.2.2. Water content determination

The hydrogels were prepared and weighed (W_0). After lyophilization, they were weighed again (W_1). The water content of the hydrogels was calculated using the following formula [34]:

$$\text{Water content (\%)} = W_0 - W_1/W_0 \times 100.$$

The water content was determined from the average values of five measurements.

2.3.2.3. Scanning electron microscopy (SEM)

The atelocollagen-based hydrogels were frozen at -80°C and lyophilized, and finally coated with gold under vacuum at 20 mA for 2 min. The surface and the cross-sectional pore size of the hydrogels were observed by SEM (Zeiss Evo 10) [21] and analyzed by Zeiss Evo 10 software.

2.3.3. Cell viability

The viability of human dermal fibroblasts encapsulated in the atelocollagen-based hydrogel was determined by live/dead cell staining. This experiment was performed with normoglycemic human dermal fibroblasts (N-HDFs) (passages 2–4). The atelocollagen-based prehydrogel solution was prepared according to the aforementioned protocol. N-HDFs at a concentration of 3.3×10^5 cells ml^{-1} were suspended in DMEM/F12 and the medium was removed by centrifugation. N-HDFs were resuspended slowly with the atelocollagen-based prehydrogel solution by using a pipette and incubated for 2.5 h at 37°C . After gelation, the cell-laden hydrogels were incubated in DMEM/F-12 medium containing 1% L-glutamine, 5% HP, 2 U ml^{-1} heparin, 1 ng ml^{-1} bFGF and 1% pen/strep for 9 d in a 5% CO_2 incubator at 37°C . The viability of the cells found in the hydrogels was evaluated by live/dead cell staining (for mammalian cells, Thermo Scientific). After the hydrogels were incubated in phenol red-free DMEM medium containing 2 mM ethidium homodimer-1 and 4 mM calcein-AM for 30 min at room temperature, they were washed with DPBS. Images were acquired with an inverted fluorescence microscope.

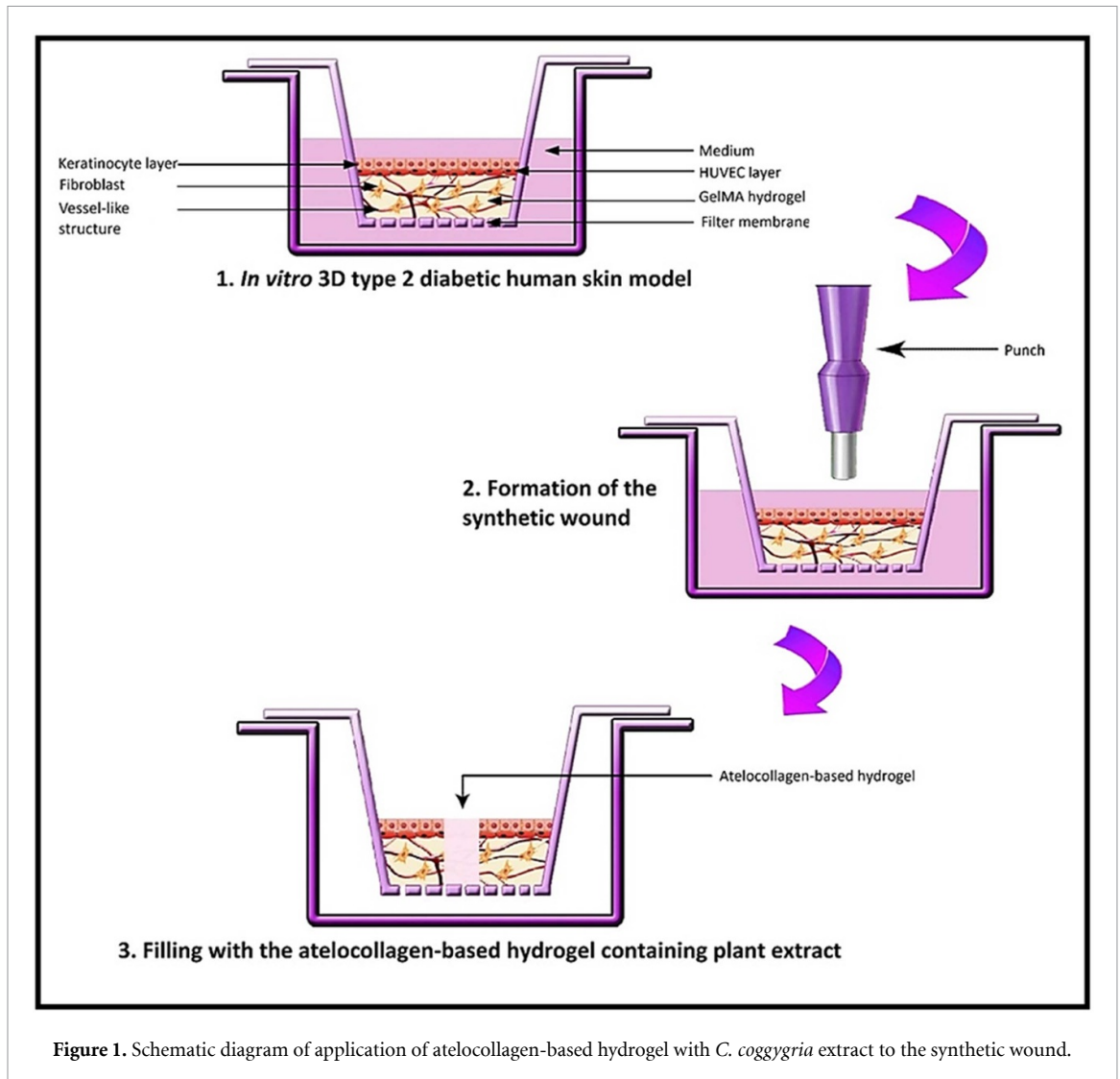
2.3.4. Determination of optimal encapsulated cell concentration

The atelocollagen-based pre-hydrogel solution was prepared according to the aforementioned protocol. N-HDFs at passages 2–4 were used for the optimization studies of hydrogels. Different concentrations of N-HDFs (3.3×10^5 , 6.7×10^5 and 8.3×10^5 cells ml^{-1}) were suspended in the prehydrogel solution and incubated for 2.5 h at 37°C . Then, the hydrogels were cultured in DMEM/F-12 medium containing 1% L-glutamine, 5% HP, 2 U ml^{-1} heparin, 1 ng ml^{-1} bFGF and 1% pen/strep for 9 d. The cell-laden atelocollagen-based hydrogels were divided into two groups; cell spreading was determined by phalloidin and DAPI staining in one of the groups, and deoxyribonucleic acid (DNA) content was measured by using a spectrophotometer (Nanodrop) to evaluate the N-HDF proliferation in the other group. For phalloidin staining, the fixed hydrogels were permeabilized with 0.1% Triton X-100 and blocked with serum for 30 min at 37°C . After blocking, the

hydrogels were incubated with phalloidin (phalloidin FITC-labeled, Sigma) for 1 h at 37°C in order to visualize the filamentous F-actin of the cells. The hydrogels were washed with DPBS, counterstained with DAPI and examined using an inverted fluorescence microscope. For the measurement of DNA content, the cell-laden hydrogels were taken into 50 $\mu\text{g ml}^{-1}$ proteinase K solution (Sigma) at day 1 and day 9, and incubated for 2 h at 37°C according to the procedure developed by Zhao *et al* [35]. After centrifugation for 10 min at 13 000 g, the supernatants were removed. Collagenase type I solution (0.1%, from *C. histolyticum*, Gibco) was added to each of the pellets and incubated in a water bath for 3.5 h at 37°C . Following centrifugation for 10 min at 13 000 g, the pellets were diluted in tris-EDTA (1XTE) solution. Then, a 1 μl sample was taken and analyzed using a spectrophotometer (Nanodrop 1000 Spectrophotometer, Thermo Scientific) at a wavelength of 260 nm to measure the amount of DNA in nanograms (ng), so the cell numbers were evaluated at the end of the first and ninth days of incubation.

2.4. Effect of atelocollagen-based hydrogel containing *C. coggygia* extracts on wound healing in *in vitro* 3D type 2 DHSM

The diabetic wound healing capacity of the treatment approaches described in sections 2.2 and 2.3 was investigated in a synthetic wound opened at the center of an *in vitro* 3D type 2 DHSM that was characterized previously. The glucose concentration was increased to 25 mM to mimic the diabetic environment [21] (figure 1). The DHSM was prepared with cells derived from type 2 diabetic patients and characterized using our previously described protocol [21]. Briefly, human dermal fibroblasts (4.5×10^6 cells ml^{-1}) and HUVECs (2.25×10^6 cells ml^{-1}) at passages 2–4 were incubated in DMEM/F-12 medium supplemented with 0.3 mg ml^{-1} atelocollagen for 20 min at 37°C , and were centrifuged at 1500 rpm for 5 min. At the same time, methacrylated gelatin (GelMA), previously synthesized and characterized in our laboratory, was diluted in DMEM/F-12 at a concentration of 8% (w/v) in an Eppendorf tube. The GelMA solution was mixed with 0.04 g ml^{-1} 2,2-Azobis(2-methyl-N-(2-hydroxyethyl) propionamide (VA 086, Wako) diluted in distilled water as a photoinitiator in order to prepare the GelMA pre-hydrogel solution. After centrifugation, the cell pellet was resuspended in GelMA prehydrogel solution, transferred to 12-well culture inserts (3 μm pores; PET membrane, Millipore) and exposed to UV A (15 W power, 368 nm wavelength, Sylvania Blacklight F15WT8/BL368) for 22 min at a distance of 5.8 cm. The HUVECs were subsequently seeded on the GelMA hydrogels at a density of 1.35×10^5 cells ml^{-1} . After incubation for 1 h at 37°C for cell attachment, the GelMA hydrogels were incubated in low-glucose DMEM (Thermo Scientific): EGM-2 media (1:1 v/v) supplemented



with 5% HP, 2 U ml⁻¹ heparin and 1% pen/strep for 24 d. At the end of incubation, keratinocytes (2.75×10^6 cells ml⁻¹) were seeded on each hydrogel and incubated in low-glucose DMEM: Cascade medium (1:1 v/v) containing 1% human keratinocyte growth supplement, 5% HP, 2 U ml⁻¹ heparin, 1 ng ml⁻¹ bFGF, 50 µg ml⁻¹ ascorbic acid (L-ascorbic acid 2-phosphate sesquimagnesium salt hydrate, Sigma) and 1% pen/strep for 7 d. After this period, the medium was changed to DMEM: DMEM/F-12 (1:1 v/v) containing 5% HP, 2 U ml⁻¹ heparin, 1 ng ml⁻¹ bFGF, 50 µg ml⁻¹ ascorbic acid and 1% pen/strep for 4 d, and the glucose concentration was increased to 25 mM in order to mimic the high blood glucose concentration of diabetic patients [36] during the following 9 d.

At the end of the incubation, the synthetic wounds were generated via biopsy punches (4 mm in diameter, Acupunch, Acuderm Inc., USA) on the DHSMs. For diabetic wound healing, the synthetic wounds were filled with atelocollagen-based hydrogel with predetermined *C. coggygia* extracts (DW and T) and then incubated at 37 °C for 2.5 h for gelation.

The treated DHSMs were incubated for 9 d in DMEM: DMEM/F-12 (1:1 v/v) media with 25 mM glucose concentration containing 5% HP, 2 U ml⁻¹ heparin, 1 ng ml⁻¹ bFGF, 50 µg ml⁻¹ ascorbic acid and 1% pen/strep in the 5% CO₂ incubator. After incubation, the treated DHSMs were washed with DPBS and fixed with 4% formaldehyde. Some of the fixed models were observed in their 3D form using a confocal microscope, while the others were snap frozen and then serially cryosectioned into 60 µm thick sections. After permeabilization with 0.1% Triton X-100, the treated DHSMs were blocked with serum for 30 min at room temperature. The treated DHSMs were incubated with 1:500 diluted anti-cytokeratin 5 to label keratinocytes, 1:100 diluted anti-vimentin to label fibroblasts, and 1:50 diluted anti-CD31 primary antibodies to label HUVECs overnight at 4 °C. At the end of the incubation period, the treated DHSMs were washed with DPBS, labeled with Alexa Fluor 488 and Alexa Fluor 568-conjugated secondary antibodies for 45 min at 37 °C and then washed with DPBS. Finally, the cell nuclei were counterstained with DAPI and the DHSMs were observed using a

confocal microscope (Zeiss LMS 700, Germany) and an inverted fluorescence microscope. Then, using the same method, the wound closure was evaluated by loading the predetermined amounts of fibroblasts into the atelocollagen-based hydrogel containing the *C. coggyria* extract that gave the best cell migration results.

2.5. Statistical analysis

All experiments were performed at least five times and the values expressed as the mean \pm standard deviation. All statistical analyses were performed using IBM SPSS for Windows version 20.0 (IBM Corp., Armonk, NY, USA). A Mann–Whitney U test was used depending on the number of comparisons. $p < 0.05$ was considered as statistically significant.

3. Results

3.1. Phenotypic characterization of dermal fibroblasts, keratinocytes and HUVECs

The third-passage fibroblasts, isolated from skin in an explant culture, were immunostained with anti-vimentin antibody, a specific marker of cells of mesenchymal origin [37]. All cells exhibited spindle-like morphology and were positive for vimentin (figure 2(a)), and thus the whole isolate was considered as a pure culture of fibroblasts.

The keratinocytes isolated from the skin of donors undergoing reduction mammoplasty surgery were characterized by immunostaining with anti-cytokeratin 5 antibodies. All of the cells showed a polygonal cobblestone shape characteristic of human keratinocytes, and were positive for cytokeratin 5 (figure 2(b)), one of the specific keratinocyte markers [38].

HUVECs were obtained enzymatically from human umbilical cords. After the second passage, the cells were immunostained for CD31, expressed on the surface of endothelial cells [39]. The cells showed a cobblestone-like shape and expressed CD31 (figure 2(c)); therefore, they were confirmed as HUVECs.

3.2. *C. coggyria* antimicrobial and cytotoxic effects

3.2.1. Antimicrobial activity

The antimicrobial activity of *C. coggyria* extracts was examined against *S. aureus*, *E. coli*, *P. aeruginosa*, *E. faecalis* and *C. albicans*, and MICs were determined (table 1).

It was observed that in particular, the M and T extracts had inhibitory effects on *S. aureus* and *E. faecalis*, but none of the *C. coggyria* extracts had an inhibitory effect on *E. coli* and *P. aeruginosa*. In addition, *C. albicans* was inhibited by all plant extracts. However, with the exception of the traditional extract, their use is hampered due to their high

MIC concentrations, which appeared to be cytotoxic to fibroblasts. A possible reason why high extract concentrations were generally effective may be the differences in the amount and types of secondary metabolites extracted by different extraction methods.

3.2.2. Cell viability

Different concentrations of *C. coggyria* extracts (H, DCM, DCM-M, M, DW, T) were applied to the T2-HDFs over 4 d to determine their cytotoxic effects. While evaluating the MTT assay results, the viability of the T2-HDFs treated with the vehicle solution for 4 d was accepted as 100%, and the percent cell viability of the cells treated with the extracts was calculated accordingly (figure 3). The cell viabilities at the beginning of the incubation (TCP^o) were used for the evaluation of cytotoxic effect of the extracts at the end of 4 d, and those of the control groups on the fourth day (TCP) were used to evaluate the cell proliferation rates. It was observed that the administration of the *C. coggyria* hexane extract to the cells at more than 150 $\mu\text{g ml}^{-1}$ concentrations caused cytotoxicity. While 150 $\mu\text{g ml}^{-1}$ concentration of H decreased the cell proliferation rate, the other concentrations did not statistically affect the cell proliferation ($p > 0.05$). The DCM extract had no cytotoxic effect. In comparison to the TCP group, it was concluded that 100 $\mu\text{g ml}^{-1}$ ($108.02 \pm 5.51\%$), 50 $\mu\text{g ml}^{-1}$ ($113.38 \pm 2.32\%$), 25 $\mu\text{g ml}^{-1}$ ($118.03 \pm 5.92\%$), 12.5 $\mu\text{g ml}^{-1}$ ($111.31 \pm 0.41\%$) and 7.8 $\mu\text{g ml}^{-1}$ ($121.41 \pm 1.04\%$) concentrations of this extract led to a statistically significant increase in cell proliferation ($p < 0.05$). *C. coggyria* dichloromethane:methanol extracts at 2000–100 $\mu\text{g ml}^{-1}$ concentrations caused cytotoxicity. DCM-M at 50 and 25 $\mu\text{g ml}^{-1}$ concentrations decreased the cell proliferation rate ($p < 0.05$) compared to TCP but was not cytotoxic. DCM-M concentrations of 12.5 and 7.8 $\mu\text{g ml}^{-1}$ concentrations did not affect the cell proliferation rate. The administration of methanol extract to the cells at 2000–150 $\mu\text{g ml}^{-1}$ concentrations caused a cytotoxic effect. While 100, 50 and 25 $\mu\text{g ml}^{-1}$ concentrations of M decreased the cell proliferation rate, 12.5 $\mu\text{g ml}^{-1}$ concentration did not have a statistically significant effect ($p > 0.05$) in comparison to the TCP group. An M concentration of 7.8 $\mu\text{g ml}^{-1}$ led to an increase in the cell proliferation rate ($109.40 \pm 5.89\%$) ($p < 0.05$). DW at more than 25 $\mu\text{g ml}^{-1}$ concentrations was cytotoxic to the T2-HDFs. While concentrations of 25 and 12.5 $\mu\text{g ml}^{-1}$ decreased the cell proliferation rate, 7.8 $\mu\text{g ml}^{-1}$ DW increased it ($121.83 \pm 6.37\%$) significantly ($p < 0.05$) compared to the control group on the fourth day. Finally, T concentrations greater than 50 $\mu\text{g ml}^{-1}$ led to a cytotoxic effect. Although 50–12.5 $\mu\text{g ml}^{-1}$ concentrations of T decreased the cell proliferation rate, no cytotoxic effects were observed at these concentrations. The cell proliferation rate at

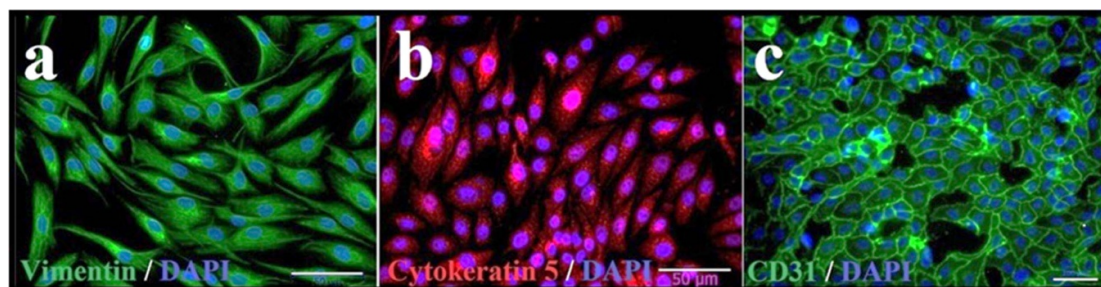


Figure 2. Fluorescence images of (a) fibroblasts, (b) keratinocytes (scale bars: 50 μm), (c) HUVECs (scale bar: 100 μm) immunostained for their specific markers.

Table 1. MIC of *C. coggyria* extracts.

Micro-organisms	MIC ($\mu\text{g ml}^{-1}$)					
	H	DCM	DCM-M	M	DW	T
<i>Staphylococcus aureus</i> ATCC 29213	—	—	500	500	2000	250
<i>Escherichia coli</i> ATCC 25922	—	—	—	—	—	—
<i>Pseudomonas aeruginosa</i> ATCC 27853	—	—	—	—	—	—
<i>Enterococcus faecalis</i> ATCC 29212	—	—	—	500	—	1000
<i>Candida albicans</i> ATCC 90028	2000	2000	1500	1500	1000	7.8

H: hexane extract; DCM: dichloromethane extract; DCM-M: dichloromethane:methanol extract; M: methanol extract; DW: distilled water extract; T: traditional extract.

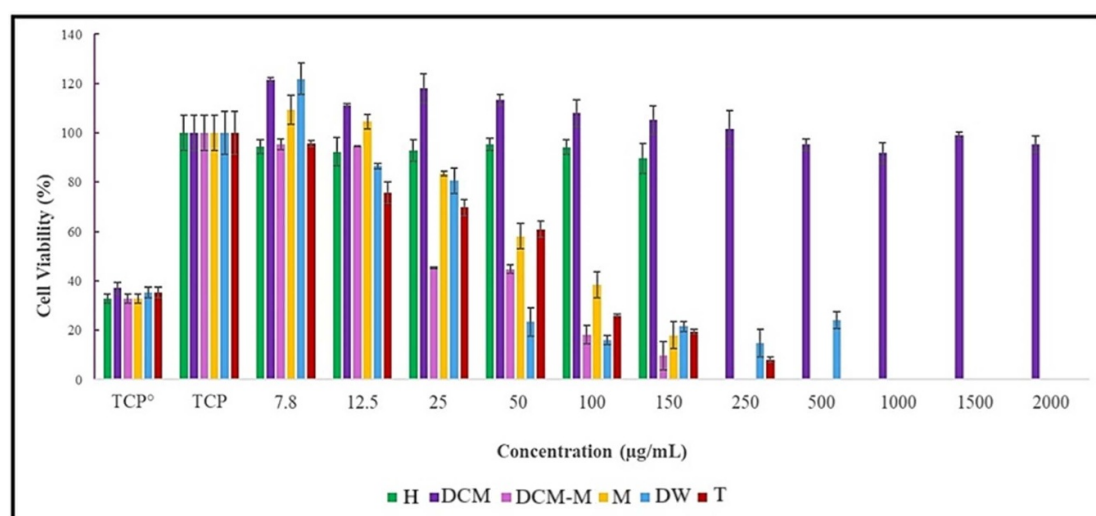


Figure 3. Cytotoxic effects of different *C. coggyria* extracts on T2-HDFs. TCP^o: control group on day 0, TCP: control group on day 4, H: hexane extract, DCM: dichloromethane extract, DCM-M: dichloromethane:methanol extract, M: methanol extract, DW: distilled water extract, T: traditional extract.

7.8 $\mu\text{g ml}^{-1}$ concentration was not significantly different from that of the TCP group ($p > 0.05$).

As a result of the cytotoxicity and antimicrobial analyses, the *C. coggyria* extracts at the lowest concentration (7.8 $\mu\text{g ml}^{-1}$) that supported the fibroblast proliferation were determined to be dichloromethane, methanol and distilled water, while the extracts that were non-cytotoxic and antifungal at the same time were 2000 $\mu\text{g ml}^{-1}$ dichloromethane and 7.8 $\mu\text{g ml}^{-1}$ traditional extract. Based on these two parameters, the best extract candidates to be used in our further studies were determined as distilled water,

as a supporter of fibroblast proliferation, and traditional extract, being antifungal and non-cytotoxic at 7.8 $\mu\text{g ml}^{-1}$ concentration.

3.3. Physical and mechanical characteristics of atelocollagen-based hydrogel

3.3.1. Physical and mechanical characteristics of prehydrogel solution

3.3.1.1. Gelation kinetics

The gelation kinetics of the prehydrogel at 37 $^{\circ}\text{C}$ were determined by a turbidity measurement at 405 nm. After 5 min of incubation at 37 $^{\circ}\text{C}$, the absorbance

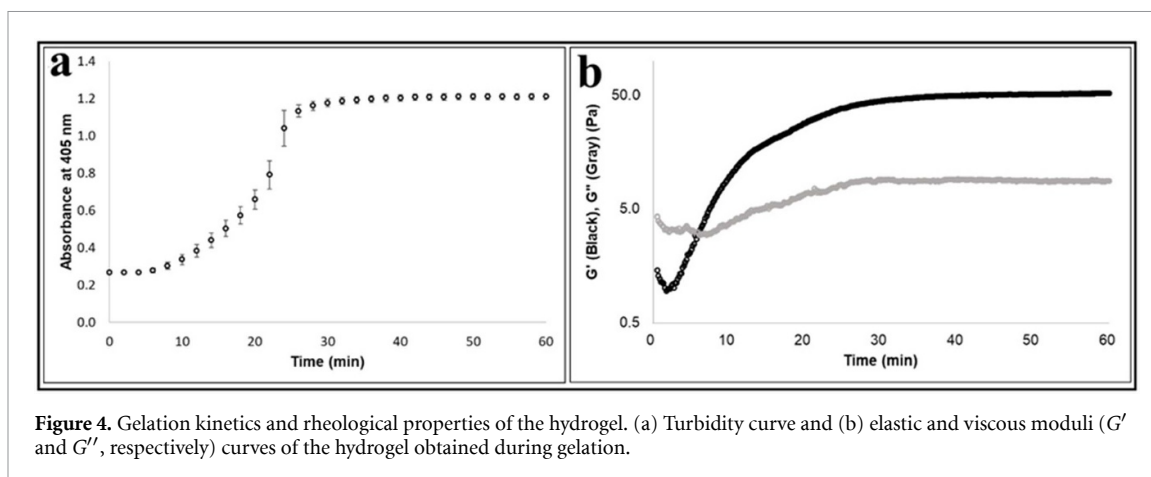


Figure 4. Gelation kinetics and rheological properties of the hydrogel. (a) Turbidity curve and (b) elastic and viscous moduli (G' and G'' , respectively) curves of the hydrogel obtained during gelation.

of the prehydrogel began to climb continuously until 30 min, when the absorbance began to stabilize, and after 45 min the absorbance of the hydrogel reached the maximum value (figure 4(a)).

3.3.1.2. Rheological properties

The crosslinking process was followed via rheological measurements; both elastic and viscous moduli (G' and G'' , respectively) were followed (at 1 Hz) as a function of time during the crosslinking reaction. A strong increase in the elastic modulus was observed, which reached a plateau at a value five times higher than the viscous modulus (52 Pa vs. 9 Pa), indicating the formation of a crosslinked network, i.e. a hydrogel (figure 4(b)).

3.3.2. Physical properties of atelocollagen-based hydrogel

Hydrogel-based wound dressings require special materials and properties, including the swelling property and water content for maintaining the water in the environment and for creating a moist environment that is beneficial to the wound-healing process, as well as the suitable pore size for enhancing the interaction with cells and the surrounding tissues [21, 34, 40]. Therefore, we investigated the physical properties of atelocollagen-based hydrogels.

In our study, the hydrogels were incubated in a growth medium at 37 °C. They reached swelling equilibrium within 24 h. The swelling ratio of the hydrogel was $27.21 \pm 4.08\%$.

To determine the water content, the hydrogel weight was measured before and after freeze-drying. The water content of the hydrogel was found to be $96.63 \pm 0.24\%$. It is thought that the high water content accelerated wound healing by preventing the wound from drying out.

The structure of the atelocollagen-based hydrogel was examined under SEM. Figure 5(a) shows that, in general, the surface of the hydrogel was not porous. Beneath this skin layer, the lower layers of the hydrogel exhibited a dense and interconnected porous

structure (figure 5(b)). The pore size of the freeze-dried hydrogel was also calculated using SEM. The average pore size of the dried hydrogel was determined as $38.75 \pm 7.67 \mu\text{m}$.

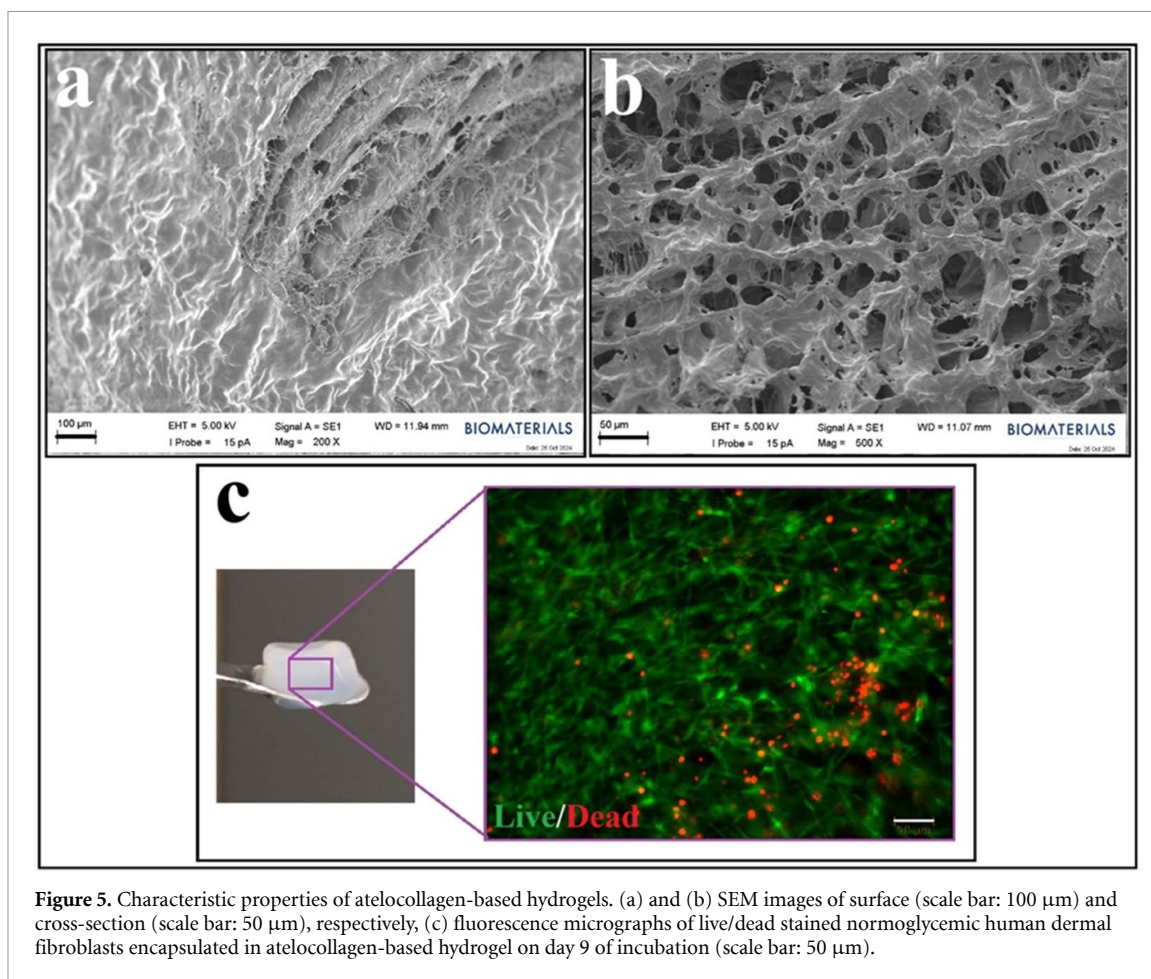
3.3.3. Cell viability

Human dermal fibroblasts were encapsulated in the atelocollagen-based hydrogel. After 9 d of incubation, the viability of the cells was assessed by live/dead assay. In this assay, calcein-AM, a membrane permeable dye, can be cleaved by the esterases within live cells to yield fluorescent calcein, producing an intense uniform green fluorescence. Ethidium homodimer-1 can only pass through the membranes of damaged cells and become fluorescent upon binding to nucleic acids, thereby producing a red fluorescence in dead cells [41]. Our live/dead staining results demonstrated a high *in vitro* viability of encapsulated N-HDFs, although the viable cells could not be enumerated due to the formation of an elongated cell network (figure 5(c)). Therefore, it was proved that the atelocollagen-based hydrogel was biocompatible.

3.3.4. Optimal cell loading concentration

Different concentrations of N-HDFs (3.3×10^5 , 6.7×10^5 and $8.3 \times 10^5 \text{ cells ml}^{-1}$) were incorporated into the atelocollagen-based hydrogel in order to determine the optimal cell concentration for the promotion of cellular growth. After 9 d of incubation, the cell-laden atelocollagen-based hydrogels were stained with phalloidin to investigate actin filament organization and thus cellular morphology. The results indicated that the N-HDFs retained their normal spindle-like morphology for up to 9 d (figures 6(a), 4(b) and 6(c)). The atelocollagen-based hydrogel containing $8.3 \times 10^5 \text{ cells ml}^{-1}$ had an extensively interconnected cellular network (figure 6(c)).

The DNA concentrations of the cell-laden atelocollagen-based hydrogels were measured by a spectrophotometer to compare the cell numbers on the first and ninth days. A significant increase in the DNA amount ($28.27 \pm 1.41\%$) was observed



only in the hydrogel inoculated with fibroblasts at a concentration of 8.3×10^5 cells ml^{-1} ($p < 0.05$) (figure 6(d)).

Based on the results of the phalloidin staining and the measurement of DNA content, 8.3×10^5 cells ml^{-1} was chosen as a suitable loading concentration for the preparation of the cell-laden hydrogel.

3.4. Wound healing effects of *C. coggygia* extracts

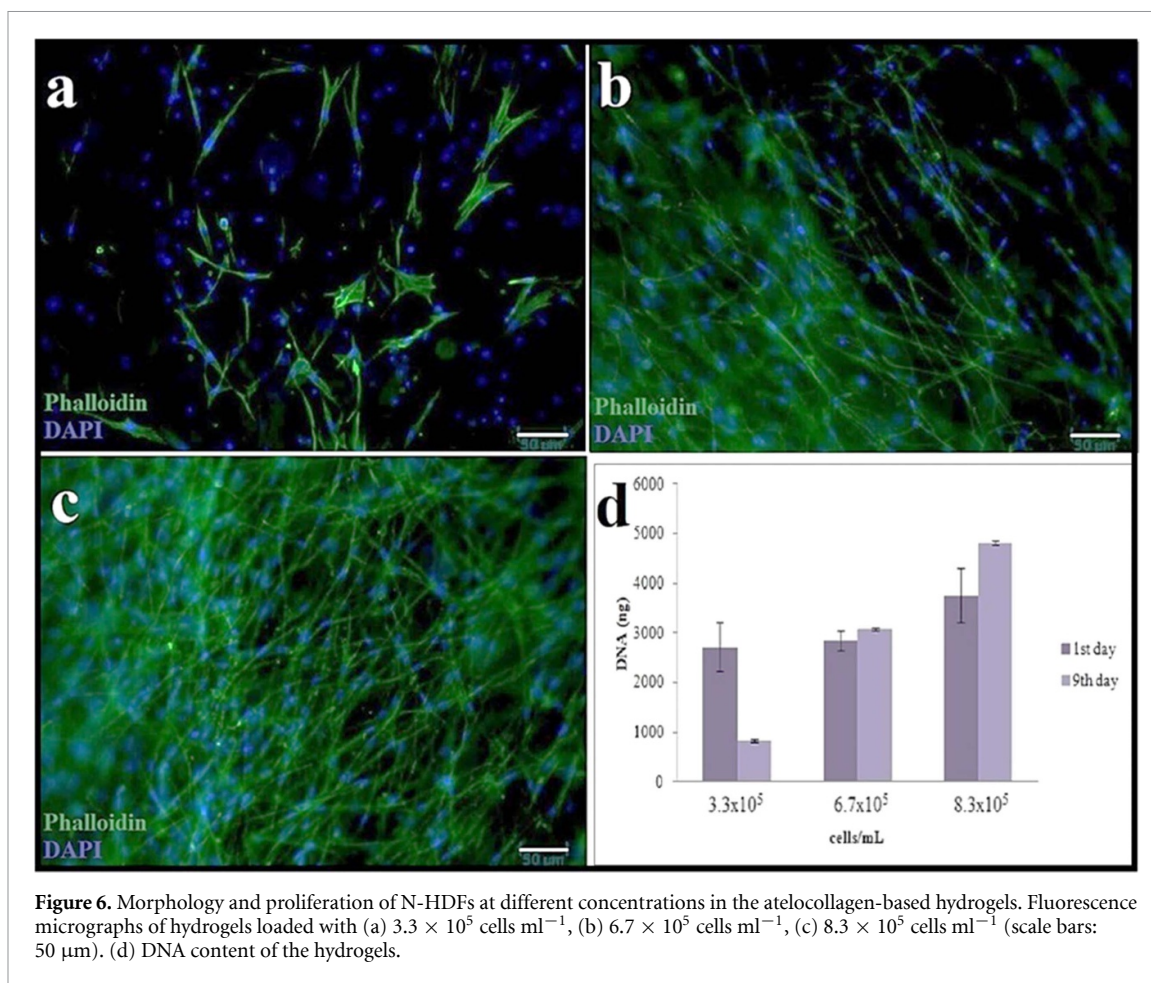
Synthetic wounds were opened on DHSMs and filled using the predetermined atelocollagen-based hydrogels containing *C. coggygia* extracts. According to our optimization studies, distilled water and traditional extracts at $7.8 \mu\text{g ml}^{-1}$ concentrations were chosen as the *C. coggygia* extracts to be used because of DW's cell proliferative effect and T's antifungal and non-cytotoxic effects. The wound healing was evaluated on the ninth day of incubation.

It was seen that the incubation period was not sufficient for closure of the wounds when both treatment approaches were examined (figures 7(a) and (b)). However, the migration of fibroblasts into the wound regions, in contrast to keratinocytes, which were few in number, was observed in both groups. Although the DW extract at $7.8 \mu\text{g ml}^{-1}$ concentration improved the fibroblast proliferation in the

2D culture (section 3.2.2), it was observed that the same concentration of T extract triggered more fibroblast migration when administered to the wound with atelocollagen-based hydrogel in 3D culture. In particular, the fibroblast migration was concentrated at the edges of the atelocollagen-based hydrogel, and the central portion was not yet completely occupied (figures 7(a) and (b)).

No vessel-like structure was observed in the wound area of any treatment group. The reason for this may be the insufficient proliferation of the fibroblast cells in the wound area, which delayed migration of the endothelial cells to this region due to the absence of ECM required for their settlement. However, it was determined that the vessel-like structures preserved their existence in both skin models until the end of the incubation period (figure 8).

In order to accelerate wound healing, the wound closure was evaluated by adding predetermined amounts of dermal fibroblasts (section 3.3.4) into the atelocollagen-based hydrogel containing the traditional extract (figure 9). At the end of the incubation period, it was observed that more keratinocytes migrated to the wound site in comparison to plain hydrogels with DW and T extracts, although the wound closure was not complete (figure 9(a)).



On the other hand, the high concentration of fibroblasts loaded to the hydrogel with T extract caused a shrinkage, which was documented in the fluorescence micrographs (figure 9(a)). In contrast to the model itself (figure 9(b)), again, no vessel-like structures were observed in the wound area.

Considering the keratinocyte and fibroblast migration, it can be concluded that the cell-laden atelocollagen-based hydrogel containing traditional extract is most effective in promoting diabetic wound healing.

4. Discussion

Diabetic wounds are severe and chronic injuries that are common in diabetic patients. Most of the presently employed wound dressings are inappropriate for treating diabetic wounds. This study aimed to develop a novel atelocollagen-based hydrogel with *C. coggyria* extract for wound healing as a new treatment approach in diabetic patients.

Most diabetic wounds have bacterial infections since hyperglycemia provides an ideal environment for the growth of micro-organisms in the wound bed [6]. In our study, the antimicrobial effects of *C. coggyria*'s different extracts were investigated against the most common sources of infection in diabetic foot

ulcers; that is, *S. aureus*, *E. faecalis*, *E. coli*, *P. aeruginosa* and *C. albicans* [27, 28]. The best reducing effect against these micro-organisms was obtained with the traditional and methanol extracts. It is known from the literature that the antimicrobial activity of compounds from plant material is usually dependent on the type of solvent used in the extraction [42]. While dichloromethane:methanol, methanol, distilled water and traditional extracts inhibited the growth of *S. aureus*, methanol and traditional extracts were observed to be effective against *E. faecalis*. Tunc *et al* [43] suggested that methanol and distilled water extracts had antibacterial activity against *S. aureus*, *E. faecalis*, *P. aeruginosa* and *E. coli*. However, their results related to the effectiveness against *P. aeruginosa* and *E. coli* and the effects of the distilled water extract against *E. faecalis* were not comparable with ours. The higher concentration of plant extracts used by the researchers may have caused this result. In the present study, all extracts inhibited the growth of *C. albicans*, but the traditional extract of *C. coggyria* at a concentration of $7.8 \mu\text{g mL}^{-1}$ showed the lowest minimum inhibitory concentration. In addition, none of the plant extracts were effective against *E. coli* and *P. aeruginosa*. The results of Singh *et al* [42] showed the antibacterial effect of the extract in methanol on *E. coli*, *P. aeruginosa* and

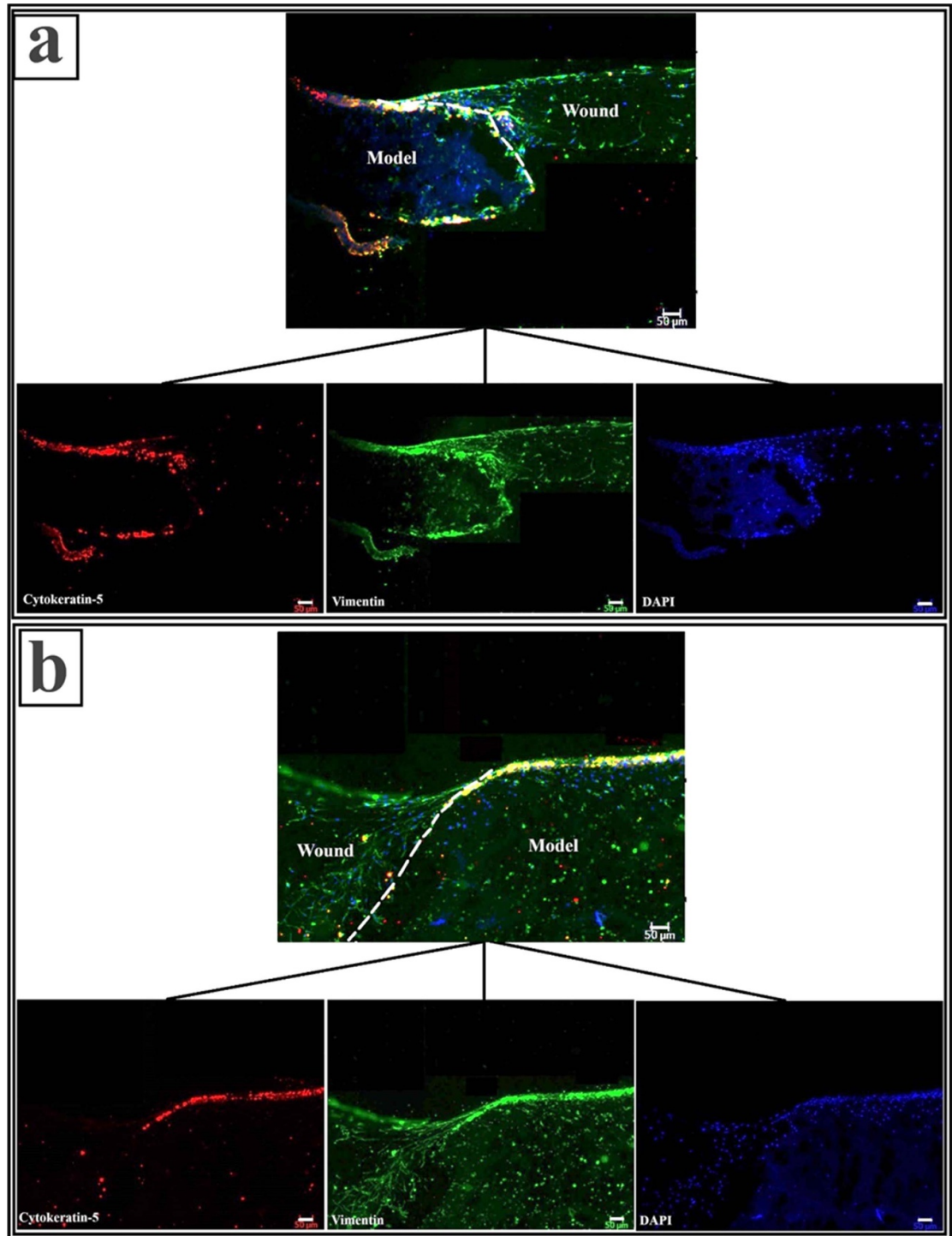


Figure 7. Fluorescence images of wound region in DHSMs on day 9 of incubation. (a) Hydrogel with DW extract, (b) hydrogel with T extract.

S. aureus, while this effect of methanol was determined against *S. aureus*, *E. faecalis* and *C. albicans* in the present study. A possible reason for this difference may be the environment in which the plant was grown, because the ingredients of secondary metabolites depend on the chemical composition of the soil, the climatic conditions of the region in which the medicinal plant grows, and the ecological situation in the area of cultivation [44]. As a result, it was shown in this study that the extracts of *C. coggygia*

had a particular effect on the growth of gram-positive bacteria and yeast, but not on gram-negative bacteria, which has an effective permeability barrier that may restrict the penetration of compounds [29]. Also, this antimicrobial effect has been attributed to the presence of large amounts of phenolic compounds in *C. coggygia* [45]. However, except for the traditional extract, the use of most of the extracts of *C. coggygia* is hampered due to their high MIC concentrations.

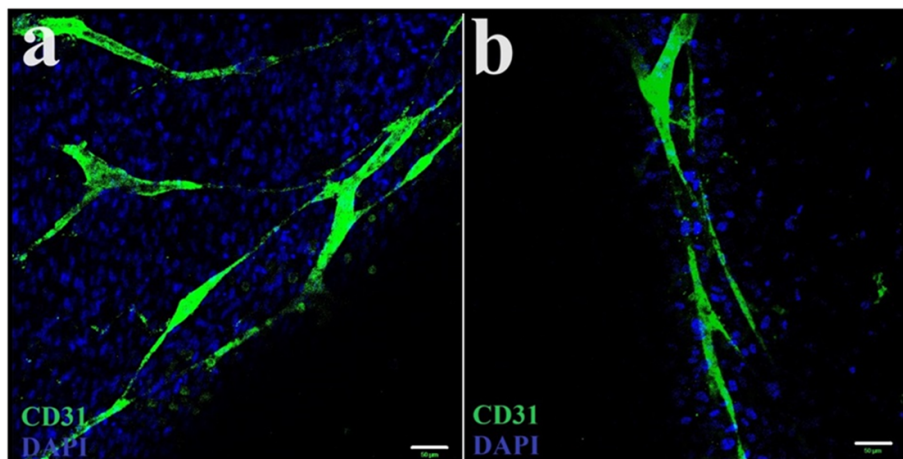


Figure 8. Confocal micrographs of vessel-like structures in DHSMs on ninth day of incubation. (a) Hydrogel with DW extract, (b) hydrogel with T extract. Scale bars: 50 μm .

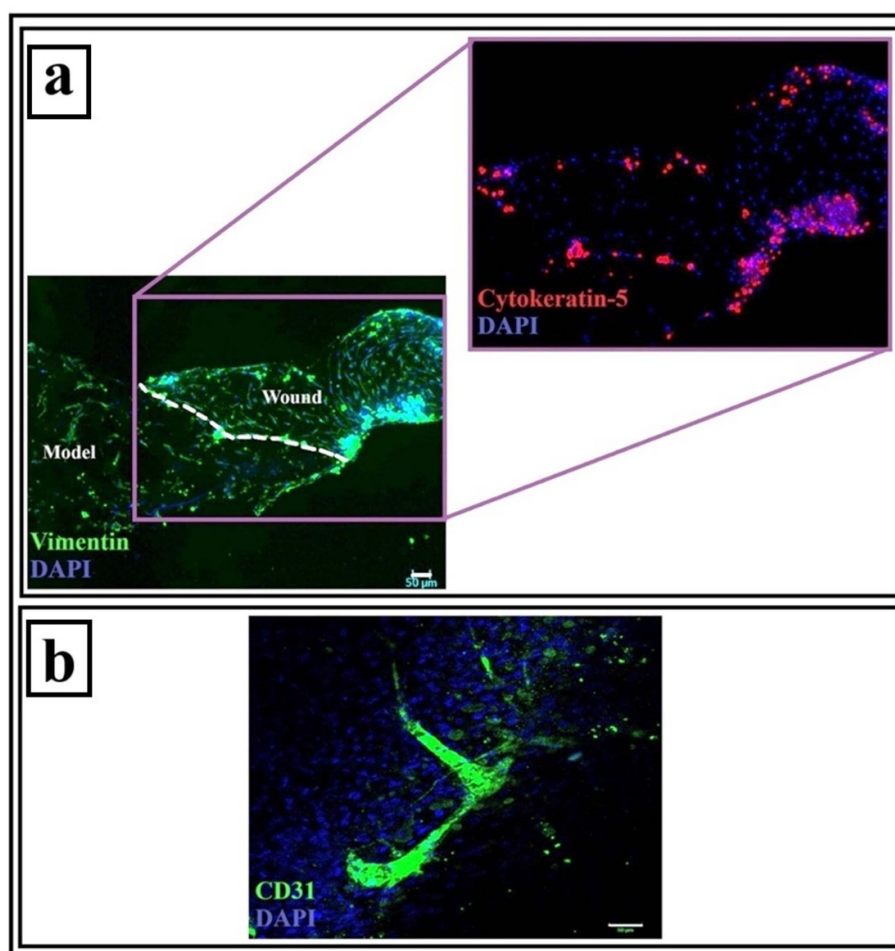


Figure 9. Fluorescence micrographs of cell-laden hydrogel with T extract on ninth day of incubation. (a) Fluorescence image of wound region, (b) confocal microscope image of vessel-like structures in DHSM. Scale bars: 50 μm .

Type 2 diabetic human dermal fibroblasts were exposed to different concentrations of *C. coggygia* extracts for 4 d in order to determine their cytotoxic effects. According to the MTT analysis results, when the minimum cytotoxic concentrations

were 250 $\mu\text{g ml}^{-1}$ of H, 100 $\mu\text{g ml}^{-1}$ of DCM-M, 150 $\mu\text{g ml}^{-1}$ of M, 50 $\mu\text{g ml}^{-1}$ of DW and 100 $\mu\text{g ml}^{-1}$ of T extract, none of the DCM concentrations were cytotoxic. Artun *et al* proved that the methanol extract of *C. coggygia* at higher than

293 $\mu\text{g ml}^{-1}$ and 1000 $\mu\text{g ml}^{-1}$ concentrations exhibited cytotoxicity in HeLa and Vero cells, respectively [46]. The reason for these deviations may be the different growing conditions of the plants, leading to different secondary metabolites [44] and used cell types. In another study, it was found that the water extract from *C. coggygia* at 5000 $\mu\text{g ml}^{-1}$ concentration was measurably inhibitory in human gingival fibroblasts and keratinocyte-like transformed cells (HaCaT cells) [45]. Our *in vitro* experiments showed similar cytotoxicity at higher concentrations of plant extracts, with the exception of dichloromethane extract, pointing out the fact that higher concentrations of plant polyphenols could be toxic [47].

Multiple infections with several kinds of bacteria worsen the condition of unhealed chronic wounds like diabetic wounds [47]. For this reason, it is important to have antimicrobial agents in wound treatment. However, these agents should also not damage the wound's resident cells. That is why the results of the antimicrobial and cytotoxicity assays were evaluated together in order to determine the most suitable plant extracts. Because none of the *C. coggygia* extracts and their different concentrations displayed antimicrobial properties for *S. aureus*, *E. coli*, *P. aeruginosa* and *E. faecalis* at the same time, the selection of the most effective extracts was based on the antifungal effect of plant extracts. It was found that antifungal and at the same time non-cytotoxic plant extracts were 7.8 $\mu\text{g ml}^{-1}$ T and 2000 $\mu\text{g ml}^{-1}$ DCM. In addition, the lowest concentrations of dichloromethane, methanol and distilled water extracts had fibroblast growth supporting effects. Therefore, according to the results of the antimicrobial and cytotoxicity analyses, T and DW at the concentration of 7.8 $\mu\text{g ml}^{-1}$ were chosen to accelerate the diabetic wound healing *in vitro*.

Severe skin defects need to be covered by wound dressings derived from various materials because they cannot heal spontaneously. Among them, hydrogels attract attention due to their ability to mimic the native skin microenvironment, due to their porous and hydrated molecular structure [48]. In addition, they are great candidates to carry active ingredients that will accelerate wound healing [6, 19]. In the present study, an atelocollagen-based hydrogel was developed as a transporter for plant extracts. Based on the physical characterization analyses, the gelation kinetics results showed that the developed hydrogel gelled in 45 min. The gelation time of thermally crosslinked collagen hydrogel varies between approximately 7.5 and 60 min depending on the temperature, hydrogel concentration and amount [49, 50]. This range is consistent with our results. Rheological analysis of the atelocollagen-based hydrogel showed that the elastic modulus was five times higher than the viscous modulus upon completion of gelation. The elastic modulus indicates the elastic response, stiffness and rigidity of the hydrogels, as the viscous modulus measures the

hydrogel's ability to flow and deform under applied stress [51]. The results represent an expansion in flexibility and a reduction in mobility of the hydrogel upon crosslinking.

The swelling behavior is used to evaluate the ability of the hydrogel to absorb the wound's leaching solution [52]. In our study, the atelocollagen-based hydrogel reached swelling equilibrium in the first 24 h. It is known from the literature [52] that rapid swelling behavior might be attributed to the porous structure of hydrogels and the presence of many hydrophilic groups, such as hydroxyl, carboxyl and amino groups. Generally, collagen-based hydrogels have a low swelling ratio, and many studies have been conducted to improve this. In a study like this, gallic acid and ellagic acid were added to the collagen hydrogel [51]. However, they could not reach the swelling ratio of the hydrogel developed in our study. A possible reason for this may be the incorporation of alginate, which has a high water retention capacity in our formulation. The water content, an important factor for creating a moist environment in the wound region, was found to be 96.63%. A moist environment promotes collagen synthesis and keratinocyte migration over the wound surface, supports the presence and function of nutrients, growth factors etc. in the wound microenvironment, facilitates autolytic debridement, and reduces pain and scarring [53]. Therefore, it was thought that the atelocollagen-based hydrogel with high water content may support wound healing when used as a wound dressing. SEM analysis of the hydrogel revealed that there were almost no pores on the surface of the hydrogel, while the lower part had a dense porous structure. The poreless upper surface accompanied by the porous lower part mimicked the structure of the skin and may control the moisture loss from the wounds to maintain a humid environment and prevent further bacterial penetration [54]. According to the cytocompatibility analysis, it was seen that most of the dermal fibroblasts were alive and formed a network due to the supporting effect of collagen on cell proliferation [55].

The dermal fibroblasts, one of the critical cell types in wound healing [56], as well as *C. coggygia* extracts, were added into the atelocollagen-based hydrogel in order to support the wound healing. All concentrations of N-HDFs loaded into the hydrogels preserved their normal spindle-like morphology. In particular, it was noted that the atelocollagen-based hydrogel containing 8.3×10^5 cells ml^{-1} had an interconnected cellular network. The amount of DNA decreased from the first day to the ninth day only in the hydrogel having the lowest fibroblast seeding concentration, 3.3×10^5 cells ml^{-1} . It is likely that the insufficient cell density in the atelocollagen-based hydrogel did not allow interaction between the cells, and so the cells migrated out of the hydrogel. The cell proliferation can be positively or negatively regulated depending on the amount

of cell–cell contact present. The highest increase in the cell number ($28.27 \pm 1.41\%$) was found in the atelocollagen-based hydrogel with a seeding concentration of 8.3×10^5 cells ml^{-1} , which was the group with the highest interconnected cellular network.

Wound healing, based on sophisticated complementary interactions between different cell types, encompasses cell adhesion, proliferation and migration, which eventually leads to highly regulated tissue regeneration [8, 35]. In our study, an *in vitro* 3D type 2 diabetic human skin wound model was treated with atelocollagen-based hydrogels containing distilled water and traditional extracts of *C. coggygia*. None of the treatments showed complete wound closure or re-epithelialization. This may be because the time adequate for cell migration *in vivo* [57] does not match the time required for the same effect *in vitro*. Hyperglycemia reduces the migratory and proliferative capabilities of keratinocytes and fibroblasts in the re-epithelialization phase. The diabetic fibroblasts and keratinocytes showed significant impairment in their migration ability [3]. Since the systemic effect of the *in vivo* environment is not present under *in vitro* conditions, this impairment may also be more pronounced. The migration of only a few keratinocytes was observed in both groups.

The normal wound healing process is based on the production, deposition and maturation of collagen. It was documented that the concentrations of collagen and hydroxyproline, which is an essential component of collagen, increased in rats during granulation tissue formation. Moreover, it has been reported in previous studies that phytochemical compounds of *C. coggygia*, such as flavonoids and terpenoids, accelerated wound healing in rats due to their astringent and antimicrobial properties [58]. In the present study, the migration of fibroblasts was present in both groups; it appeared to be more intense and even in the atelocollagen-based hydrogel containing the traditional extract of *C. coggygia*. Although the distilled water extract better promoted the fibroblast proliferation in 2D culture, it was observed that in 3D culture, the traditional extract triggered the fibroblast migration more than the distilled water extract. It is known that hydrogels as wound dressings provide a 3D architecture for cell migration and tissue regeneration [6]. The presence of collagen, ascorbic acid and sodium alginate in the used hydrogel may also have positively affected the fibroblast migration because of their properties such as stimulating collagen synthesis [59], increasing cell migration, adhesion and proliferation, and providing a moist environment favorable for re-epithelialization and rapid granulation during wound healing [60]. While vessel-like structures were present in both DHSMs, they were not seen in any of the wound regions. The probable reasons for this may be that the fibroblasts could not migrate sufficiently to pave the way for HUVEC migration to the wound area, and the production of ECM

was not sufficient for the relocation of endothelial cells because an imbalance between MMPs and their inhibitors (TIMPs) leads to impaired cell migration and reduced collagen synthesis under diabetic conditions. In addition, cell signaling between fibroblasts and endothelial cells is critical for vascularization, and impaired angiogenesis underlying diabetic wounds occurs when the signaling goes awry [3].

Fibroblasts are critical in supporting wound healing as they are involved in key processes such as breaking down fibrin clots, and creating new ECM and collagen structures to support the other cells associated with effective wound healing and contracting the wound [56]. Basal cells in the epidermal layer proliferate from the wound edges and interact with the framework of the ECM created by myofibroblasts, which differentiate from fibroblasts. Keratinocytes are unable to migrate and formally epithelialize the wounds in the absence of proper signaling intermediates and myofibroblast functionality. This is because keratinocytes need a basal lamina on which to migrate [61]. In the last part of this study, predetermined amount of fibroblasts was loaded into the atelocollagen-based hydrogel containing the traditional extract, which showed higher fibroblast migration during the *in vitro* diabetic wound healing. Although wound closure could not be achieved completely and no new vessel-like structures were observed at the wound edges, the migration of more keratinocytes to the wound area was seen. Compared to the other two groups, the hydrogel at the wound site shrank because of the high fibroblast load.

5. Conclusion

In this study, a novel wound dressing was developed from atelocollagen-based hydrogel containing *C. coggygia* extract for diabetic wound healing. While dichloromethane, methanol and distilled water extracts at the lowest concentrations supported the fibroblast proliferation among six different *C. coggygia* extracts, 2000 $\mu\text{g ml}^{-1}$ dichloromethane and 7.8 $\mu\text{g ml}^{-1}$ traditional extracts had both non-cytotoxic and antimicrobial effects. In general, it was determined that high concentrations of *C. coggygia* extracts were especially effective on yeast and gram-positive bacteria but not on gram-negative bacteria. Sodium alginate and ascorbic acid were blended with atelocollagen derived from bovine tendons, and the hydrogels were obtained by thermal crosslinking at 37 °C. The characteristic properties of the hydrogel, such as the pore size, water content and swelling ratio, were found to be suitable for use as a wound dressing. The wound healing properties of *C. coggygia* extract containing hydrogels were demonstrated on artificial wounds opened at the center of an *in vitro* 3D type 2 DHSM. Although the incubation period was not sufficient for closure of the wounds, fibroblast, but not keratinocyte, migration to the wound region

was observed. When the fibroblasts were loaded into the atelocollagen-based hydrogel, more keratinocytes migrated to the wound region. The fibroblast-laden atelocollagen-based hydrogel with *C. coggygia* traditional extract needs to be tested in a diabetic animal model to evaluate its effectiveness under *in vivo* conditions, where its systemic effect can also be observed.

Data availability statement

All data that support the findings of this study are included within the article (and any supplementary files).

Acknowledgment

The authors would like to thank Dr Deniz Yucel, from Acibadem University, for her help in obtaining confocal microscopy images and Dr Canan Sevimli Gur, from Izmir Katip Celebi University, for her guidance on the preparation of plant extracts. This research was supported by a Grant (No. 2015/045) from Kocaeli University.

Ethical statement

All protocols involving donors were conducted in adherence with the Declaration of Helsinki. Approval was received from the Kocaeli University Medical Ethics Committee for the human-derived tissue samples used in this research, and all procedures followed were in accordance with its guidelines (protocol code: KOU KAEK 2015/236). Informed consent was obtained from all identifiable donors, who are also aware of the intended publication.

ORCID iDs

Candan Yilmaz Ozdogan  <https://orcid.org/0000-0001-5885-4189>

Halime Kenar  <https://orcid.org/0000-0003-0433-5513>

References

- [1] Chen J, Qin S, Liu S, Zhong K, Jing Y, Wu X, Peng F, Li D and Peng C 2023 Targeting matrix metalloproteases in diabetic wound healing *Front. Immunol.* **14** 1089001
- [2] Song J, Zhang Y, Chan S Y, Du Z, Yan Y, Wang T, Li P and Huang W 2021 Hydrogel-based flexible materials for diabetes diagnosis, treatment, and management *npj Flex. Electron.* **5** 1–17
- [3] Phang S J, Arumugam B, Kuppusamy U R, Fauzi M B and Looi M L 2021 A review of diabetic wound models—novel insights into diabetic foot ulcer *J. Tissue Eng. Regen. Med.* **15** 1051–68
- [4] Mariadoss A V A, Sivakumar A S, Lee C H and Kim S J 2022 Diabetes mellitus and diabetic foot ulcer: etiology, biochemical and molecular based treatment strategies via gene and nanotherapy *Biomed. Pharmacother.* **151** 113134
- [5] Liu I P *et al* 2022 Angiogenesis-based diabetic skin reconstruction through multifunctional hydrogel with sustained releasing of M2 macrophage-derived exosome *Chem. Eng. J.* **431** 132413
- [6] Gao D, Zhang Y, Bowers D T, Liu W and Ma M 2021 Functional hydrogels for diabetic wound management *APL Bioeng.* **5** 031503
- [7] Chai C, Zhang P, Ma L, Fan Q, Liu Z, Cheng X, Zhao Y, Li W and Hao J 2023 Regenerative antibacterial hydrogels from medicinal molecule for diabetic wound repair *Bioact. Mater.* **25** 541–54
- [8] Holl J, Kowalewski C, Zimek Z, Fiedor P, Kaminski A, Oldak T, Moniuszko M and Eljaszewicz A 2021 Chronic diabetic wounds and their treatment with skin substitutes *Cells* **10** 655
- [9] Guan Y, Niu H, Liu Z, Dang Y, Shen J, Zayed M, Ma L and Guan J 2021 Sustained oxygenation accelerates diabetic wound healing by promoting epithelialization and angiogenesis and decreasing inflammation *Sci. Adv.* **7** eabj0153
- [10] Matic S, Stanic S, Mihailovic M and Bogojevic D 2016 *Cotinus coggygia* Scop.: an overview of its chemical constituents, pharmacological and toxicological potential *Saudi J. Biol. Sci.* **23** 452–61
- [11] Majewska I and Gendaszewska-Darmach E 2011 Proangiogenic activity of plant extracts in accelerating wound healing- a new face of old phytomedicines *Acta Biochim. Pol.* **58** 449–60
- [12] Matic S *et al* 2011 Extract of the plant *Cotinus coggygia* Scop. Attenuates pyrogallol-induced hepatic oxidative stress in Wistar rats *Can. J. Physiol. Pharmacol.* **89** 401–11
- [13] Novakovic M, Vučković I, Janačković P, Soković M, Filipović A, Tešević V and Milosavljević S 2007 Chemical composition, antibacterial and antifungal activity of the essential oils of *Cotinus coggygia* from Serbia *J. Serb. Chem. Soc.* **72** 1045–51
- [14] Deniz F S S, Salmes R E, Emerce E, Cankaya I I T, Yusufoglu H S and Orhan I E 2020 Evaluation of collagenase, elastase and tyrosinase inhibitory activities of *Cotinus coggygia* Scop. through *in vitro* and *in silico* approaches *South Afr. J. Bot.* **132** 277–88
- [15] You H J and Han S K 2014 Cell therapy for wound healing *J. Korean Med. Sci.* **29** 311–9
- [16] Han S K, Kim H S and Kim W K 2009 Efficacy and safety of fresh fibroblast allografts in the treatment of diabetic foot ulcers *Dermatologic Surg.* **35** 1342–8
- [17] You H J, Han S K and Rhie J W 2014 Randomised controlled clinical trial for autologous fibroblast-hyaluronic acid complex in treating diabetic foot ulcers *J. Wound Care* **23** 521–30
- [18] Hanft J R and Surprenant M S 2002 Healing of chronic foot ulcers in diabetic patients treated with a human fibroblast-derived dermis *J. Foot Ankle Surg.* **41** 291–9
- [19] Pérez-Rafael S, Ivanova K, Stefanov I, Puiggali J, Del Valle L J, Todorova K, Dimitrov P, Hinojosa-Caballero D and Tzanov T 2021 Nanoparticle-driven self-assembling injectable hydrogels provide a multi-factorial approach for chronic wound treatment *Acta Biomater.* **134** 131–43
- [20] Mathew-Steiner S S, Roy S and Sen C K 2021 Collagen in wound healing *Bioengineering* **8** 63
- [21] Yilmaz Ozdogan C, Kenar H, Davun K E, Yucel D, Doger E and Alagoz S 2020 An *in vitro* 3D diabetic human skin model from diabetic primary cells *Biomed. Mater.* **16** 015027
- [22] Ibusuki S, Halbesma G J, R. andolph M A, Redmond R W, Kochevar I E and Gill T J 2007 Photochemically cross-linked collagen gels as three-dimensional scaffolds for tissue engineering *Tissue Eng.* **13** 1995–2001
- [23] Ma G, Fang D, Liu Y, Zhu X and Nie J 2012 Electrospun sodium alginate/poly(ethylene oxide) core-shell nanofibers scaffolds potential for tissue engineering applications *Carbohydr. Polym.* **87** 737–43
- [24] Wang L, Shelton R M, Cooper P R, Lawson M, Triffitt J T and Barralet J E 2003 Evaluation of sodium alginate for bone marrow cell tissue engineering *Biomaterials* **24** 3475–81

- [25] Sun M, Xie Q, Cai X, Liu Z, Wang Y, Dong X and Xu Y 2020 Preparation and characterization of epigallocatechin gallate, ascorbic acid, gelatin, chitosan nanoparticles and their beneficial effect on wound healing of diabetic mice *Int. J. Biol. Macromol.* **148** 777–84
- [26] Kenar H, Yilmaz Ozdogan C, Dumlu C, Doger E, Kose G T and Hasirci V 2019 Microfibrous scaffolds from poly(L-lactide-co-ε-caprolactone) blended with xeno-free collagen/hyaluronic acid for improvement of vascularization in tissue engineering applications *Mater. Sci. Eng. C* **97** 31–44
- [27] Monami M, Scatena A, Schlecht M, Lobmann R, Landi L, Ricci L and Mannucci E 2020 Antimicrobial photodynamic therapy in infected diabetic foot ulcers *J. Am. Podiatric Med. Assoc.* **110** 1–6
- [28] Pickwell K, Geerts M, Von Moorsel D, Hilkman D, Kars M and Schaper N C 2020 Regional differences in cell-mediated immunity in people with diabetic peripheral neuropathy *Diabetic Med.* **37** 350–5
- [29] Marčetić M, Božić D, Milenković M, Malešević N, Radulović S and Kovačević N 2013 Antimicrobial, antioxidant and anti-inflammatory activity of young shoots of the smoke tree, *Cotinus coggygria* *Scop Phytother. Res.* **27** 1658–63
- [30] Muniandy K, Gothai S, Tan W S, Kumar S S, Esa N M, Chandramohan G, Al-Numair K S and Arulselvan P 2018 *In vitro* wound healing potential of stem extract of *Alternanthera sessilis* *J. Evid. Based Complementary Altern. Med.* **2018** 1–13
- [31] Jeong W, Kim M K and Kang H W 2021 Effect of detergent type on the performance of liver decellularized extracellular matrix-based bio-inks *J. Tissue Eng.* **12** 2041731421997091
- [32] Vulpe R, Le Cerf D, Dulong V, Popa M, Peptu C, Verestiuc L and Picton L 2016 Rheological study of *in-situ* crosslinkable hydrogels based on hyaluronan acid, collagen and sericin *Mater. Sci. Eng. C* **69** 388–97
- [33] Wan W, Cai F, Huang J, Chen S and Liao Q 2019 Skin-inspired 3D bilayer scaffold enhances granulation tissue formation and anti-infection for diabetic wound healing *J. Mater. Chem. B* **7** 2954–61
- [34] Shen X, Zhao D, Shi J, Li C, Bai Y, Qiu L, Xuan Y and Wang J 2024 Copper peroxide loaded gelatin/oxide dextran hydrogel with temperature and pH responsiveness for antibacterial and wound healing activity *Int. J. Biol. Macromol.* **274** 133258
- [35] Zhao X, Sun X, Yildirim L, Lang Q, Lin Z Y (William), Zheng R, Zhang Y, Cui W, Annabi N and Khademhosseini A 2017 Cell infiltrative hydrogel fibrous scaffolds for accelerated wound healing *Acta Biomater.* **49** 66–77
- [36] Vincent A M, Edwards J L, McLean L L, Hong Y, Cerri F, Lopez I, Quattrini A and Feldman E L 2010 Mitochondrial biogenesis and fission in axons in cell culture and animal models of diabetic neuropathy *Acta Neuropathol.* **120** 477–89
- [37] Liu X, Zhang R, Shi H, Li X, Li Y, Taha A and Xu C 2018 Protective effect of curcumin against ultraviolet A irradiation-induced photoaging in human dermal fibroblasts *Mol. Med. Rep.* **17** 7227–37
- [38] Chavez-Munoz C, Nguyen K T, Xu W, Hong S J, Mustoe T A and Galiano R D 2013 Transdifferentiation of adipose-derived stem cells into keratinocyte-like cells: engineering a stratified epidermis *PLoS One* **8** e80587
- [39] Quarumby S, Kumar P, Wang J, Macro J A, Hutchinson J J, Hunter R D and Kumar S 1999 Irradiation induces upregulation of CD31 in human endothelial cells, Atherosclerosis *Thrombosis Vasc. Biol.* **19** 588–97
- [40] Gao Q et al 2019 3D printing of complex GelMA-based scaffolds with nanoclays *Biofabrication* **11** e035006
- [41] Zhou S, Cui Z and Urban J 2011 *Dead Cell Counts during Serum Cultivation are Underestimated by the Fluorescent Live/dead Assay* vol 6 (WILEY-VCH Verlag) pp 513–8
- [42] Singh S K, Vishnoi R, Dhingra G K and Kishor K 2012 Antibacterial activity of leaf extracts of some selected traditional medicinal plants of Uttarakhand, North East India *J. Appl. Nat. Sci.* **4** 47–50
- [43] Tunc K, Hos A and Gunes B 2013 Investigation of antibacterial properties of *Cotinus coggygria* from Turkey *Pol. J. Environ. Stud.* **22** 1559–61
- [44] Sukhikh S, Noskova S, Pungin A, Ivanova S, Skrypnik L, Chupakhin E and Babich O 2021 Study of the biologically active properties of medicinal plant *Cotinus coggygria* *Plants* **10** 1224
- [45] Ferrazzano G F, Roberto L, Catania M R, Chiaviello A, De Natale A, Roscetto E, Pinto G, Pollio A, Ingenito A and Palumbo G 2013 Screening and scoring of antimicrobial and biological activities of Italian vulnerable plants against major oral pathogenic bacteria *Evid. Based Complement Alternat Med.* **2013** 1–10
- [46] Artun F T, Karagoz A, Ozcan G, Melikoglu G, Anil S, Kultur S and Sutlupinar N 2016 *In vitro* anticancer and cytotoxic activities of some plant extracts on HeLa and Vero cell lines *J. BUON.* **21** 720–5
- [47] Michalowska A G, Abramowski Z, Jovel E and Hes M 2008 Antioxidant potential of herbs extracts and impact on HEPG2 cells viability *Acta Sci. Pol. Technol. Alim.* **7** 61–72
- [48] Tavakoli S and Klar A S 2020 Advanced hydrogels as wound dressings *Biomolecules* **10** 1169
- [49] Buitrago J O, Patel K P, El-Fiqi A, Lee J H, Kundu B, Lee H H and Kim H W 2018 Silk fibroin/collagen protein hybrid cell-encapsulating hydrogels with tunable gelation and improved physical and biological properties *Acta Biomater.* **69** 218–33
- [50] Furusawa K, Sato S, Masumoto J-I, Hanazaki Y, Maki Y, Dobashi T, Yamamoto T, Fukui A and Sasaki N 2011 Studies on the formation mechanism and the structure of the anisotropic collagen gel prepared by dialysis-induced anisotropic gelation *Biomacromolecules* **13** 29–39
- [51] Munir S, Yue W, Li J, Yu X, Ying T, Liu R, You J, Xiang S and Hu Y 2023 Effects of phenolics on the physicochemical and structural properties of collagen hydrogel *Polymers* **15** 4647
- [52] Xin C, Cheng Z, Liu W, Li W and Zhu H 2024 The antibacterial and hemostatic activity of *Gastrodia elata* polysaccharide-based hydrogel embedded with drug-carrying microspheres accelerates diabetic wound healing *Chem. Eng. J.* **492** 152403
- [53] Nuutila K and Eriksson E 2021 Moist wound environment with commonly available dressings *Adv. Wound Care* **10** 685–98
- [54] Li Y, Zhu C, Fan D, Fu R, Ma P, Duan Z, Li X, Lei H and Chi L 2019 A bilayer PVA/CMC/PEG hydrogel with gradually changing pore sizes for wound dressing *Macromol. Biosci.* **19** 1800424
- [55] Grunert P, Borde B H, Towne S B, Moriuchi Y, Hudson K D, Bonassor L J and Härti R 2015 Riboflavin crosslinked high-density collagen gel for the repair of annual defects in intervertebral discs: an *in vivo* study *Acta Biomater.* **26** 215–24
- [56] Bainbridge P 2013 Wound healing and the role of fibroblasts *J. Wound Care* **22** 407–12
- [57] Tsuboi R, Shi C, Rifkin D B and Ogawa H 1992 A wound healing model using healing-impaired diabetic mice *J. Dermatol.* **19** 673–5
- [58] Aksoy H, Sancar M, Sen A, Okuyan B, Bitis L, Uras F, Akakin D, Cevik O, Kultur S and İzzettin F V 2016 The effect of topical ethanol extract of *C. coggygria* Scop. on cutaneous wound healing in rats *Nat. Prod. Res.* **30** 452–5
- [59] Michel M, L'heureux N, Pouliot R, Xu W, Auger F A and Germain L 1999 Characterization of a new tissue-engineered human skin equivalent with hair *In vitro Cell Dev. Biol. Animal* **35** 318–26
- [60] Kaur G, Narayanan G, Garg D, Sachdev A and Matai I 2022 Biomaterials-based regenerative strategies for skin tissue wound healing *ACS Appl. Bio Mater.* **5** 2069–106
- [61] Wan R, Weissman J P, Grundman K, Lang L, Grybowski D J and Galiano R D 2021 Diabetic wound healing: the impact of diabetes on myofibroblast activity and its potential therapeutic treatments *Wound Repair Regen.* **29** 573–81